RSC Advances

PAPER

View Article Online
View Journal | View Issue

Cite this: *RSC Adv.*, 2025, **15**, 4546

Ratiometric discrimination of Th^{4+} ions by a fluorogenic quinoline appended phenanthridine sensor and its applications†

Selin Manoj Kumar,[a] Sathishkumar Munusamy,[b] Saravanan Enbanathan,[a] Sivaranjani Ranganadin[a] and Sathiyanarayanan Kulathu Iyer *[a]

Received 17th December 2024
Accepted 3rd February 2025

DOI: 10.1039/d4ra08840a

rsc.li/rsc-advances

A new phenanthridine appended quinoline-based chemoreceptor 5-(5-(quinolin-8-yl)thiophen-2-yl)-tetrahydrodibenzo[a,i]phenanthridine (**PHQBA**) was successfully synthesized and characterized by ^{1}H, ^{13}C, and HRMS spectral analyses. The promising chelation-induced process in **PHQBA** was accelerated by Th^{4+} ions, which impart robust ratiometric green fluorescence at 515 nm. The host–guest complex formed in a 1 : 1 binding stoichiometry between Th^{4+} ions and **PHQBA** was demonstrated by Jobs plot experiments. The Benesi–Hildebrand (BH) plot was employed to compute the binding constant for the complexation of **PHQBA** + Th^{4+}, which was determined to be 3.77×10^{5} M^{-1}. To comprehend the detection mechanism of **PHQBA**, DFT, and TDDFT, eased computational studies were conducted and well supported by the experimental results. Moreover, the limit of detection (LOD) of **PHQBA** was determined as 223 nM, which defines the remarkable optical sensitivity of the sensor **PHQBA**. Further, portable paper strip detection and real-time determination of Th^{4+} ions in real water samples ensure the practical applications of **PHQBA**.

Introduction

Thorium is a potentially important radioactive metal in the earth's crust that is extensively used in modern industrial platforms.[1] It has plenty of applications in the formulation of lantern mantles, lenses, carbon lamps, ceramics, and welding appliances.[2] Since thorium exists in a +4-oxidation state, most nuclear fuel recycling is accomplished in a medium with high acidity.[3,4] Undesirably, thorium ions create serious contamination in waterbodies such as seas, lakes, and rivers which immensely affects living creatures. Also, the toxicity of thorium ions can cause renal injury and dermatitis.[5] According to the reports of the World Health Organisation (WHO), the permissible limit of thorium is 0.6 μg per kg per day.[6] Therefore, there is a need to develop a precise method for the quantification of thorium ions. Many spectroanalytical techniques are available, but it can be challenging to identify target analytes due to their complex operating procedures. Examples of these techniques include electrothermal atomic absorption spectroscopy (ETASS),[7] inductively coupled plasma emission spectroscopy (ICP-AES),[8] accelerator mass spectrometry (AMS),[9] laser ablation microprobe mass analyzer (LAAMA),[10] atomic absorption spectroscopy (AAS)[11] and neutron activation analysis (NAA).[12] While comparing these approaches, fluorescent sensing is an emerging alternative to conventional methods[13–18] for the detection of analytes due to their selectivity, sensitivity, rapid response, and ease of access. Detection of heavy metal ions follows various photochemical mechanisms including Forster resonance energy transfer (FRET),[19] intramolecular charge transfer (ICT),[20] exited state intramolecular charge transfer (ESIPT),[21] and twisted intramolecular charge transfer (TICT).[22] Among all these photochemical processes, chelation enhanced fluorescence process predominantly produces a well-defined spectral response that accelerates sensitive ratiometric detection of analytes.[23–30] Due to the well-functionalized design[31,32] of phenanthridine-based chemosensing systems, it has gained significant attention, which plays a vital role in spectroscopic properties. The advantages of these sensors include bright emission,[33] large Stokes shift,[34] and ease of emission wavelength modulation[35,36] upon analyte interaction. These features are necessary for the rational construction of ratiometric sensors. While comparing turn-on and turn-off fluorescent probes, ratiometric chemosensors could provide precise calibration by decoding dual emission ratio signals, which could improve the sensitivity with great accuracy during the determination of target analytes.[37–41] Hence, designing a ratiometric fluorescent sensor to identify Th^{4+} ions with greater sensitivity and selectivity is crucial. In our group, phenanthridine-derived chemosensors have recently been employed as effective tools for

[a]*Department of Chemistry, School of Advanced Sciences and Vellore Institute of Technology, Vellore-632014, India. E-mail: sathiya_kuna@hotmail.com*

[b]*Department of Chemistry, University of Missouri-Columbia, Columbia, MO, USA. E-mail: pra3sat@gmail.com*

† Electronic supplementary information (ESI) available. See DOI: https://doi.org/10.1039/d4ra08840a

the selective detection of thorium ions. These sensors exhibit a turn-on fluorescence response[42–44] upon interaction with thorium ions, enabling low detection limits. Ratiometric fluorescent probes are particularly advantageous as they provide signal ratios, enhancing the dynamic range and offering built-in correction for environmental effects. The observed emission color change is valuable for ratiometric fluorescence detection. To improve the optical performance of the sensor, we have rationally incorporated quinoline conjugation into the phenanthridine system. In our endeavor to develop a novel phenanthridine-derived ratiometric thorium ion sensor, **PHQBA** has been constructed. In the detection process, the chelation of heavy metal (Th^{4+}) to the electron-rich **PHQBA** ligand, results in the formation of a new **PHQBA** + Th^{4+} complex. As a result, ratiometric fluorescence has been accomplished. Fascinatingly, the sensor **PHQBA** exclusively detects Th^{4+} ions even in the presence of other cations, thereby ensuring anti-interference properties. The detection mechanism of **PHQBA** is well strengthened by DFT, HRMS, and NMR titration experiments. Further, the Jobs plot and Benesi–Hildebrand (B–H) plot depict the binding stoichiometry and association constant of Th^{4+} ions. On account of their greater emission properties, portable fluorescent paper strips were exploited for the selective and sensitive discrimination of Th^{4+} ions. In addition, Th^{4+} ions were successfully detected in environmental water samples with excellent recovery.

Results and discussion

Design and synthesis of PHQBA

In general, phenanthridine-based fluorescent sensors possess well-defined spectral responses, which is highly advantageous for analyte detection owing to their ability to hinder the self-absorption and inner filtering effects.[45–47] The designing of a thiophene-appended quinoline moiety to the phenanthridine system facilitates the chelation-enhanced fluorescence (CHEF) process with Th^{4+} ions. As shown in Scheme 1, the design of the chemoreceptor **PHQBA** includes two steps. In step one, compound **1a** was successfully synthesized by the reaction of 5-bromo-2-thiophenecarboxaldehyde and 2-tetralone. Finally, quinoline moiety was introduced to the phenanthridine system by a Suzuki coupling reaction to extend the conjugation of the phenanthridine system (**PHQBA**) for achieving ratiometric fluorescence detection (Scheme 1). The compounds were characterized by ^{1}H, ^{13}C NMR, and HRMS analyses (Fig. S1–S5†).

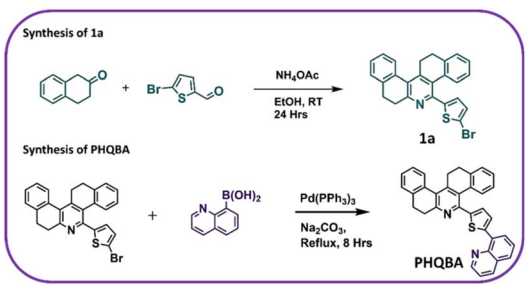

Scheme 1 Synthesis of sensor PHQBA.

Absorption studies of PHQBA

Optical selectivity is considered to be a crucial tool for the evaluation of a chemosensor. In this regard, the influence of absorption on the detection properties of **PHQBA** was initially inspected in the presence of various cation solutions such as Ca^{2+}, Ba^{2+}, Al^{3+}, Cd^{2+}, Cu^{2+}, Th^{4+}, Co^{2+}, Fe^{2+}, Fe^{3+}, Hg^{2+}, Ni^{2+}, Cr^{3+}, Pb^{2+}, Pd^{2+} Zn^{2+} La^{3+}, and Yb^{3+} in ACN/H_2O (8 : 2 v/v). As illustrated in Fig. 1a, **PHQBA** displayed an explicit absorption band at 278 and 380 nm, which could be accredited to π–π* and n–π* electronic transition respectively. Competitive cations have no significant impact on the absorption of **PHQBA**. However, the introduction of the Th^{4+} ion to the **PHQBA** solution resulted in the appearance of a new hypsochromic absorption band at 312 nm. The resulting absorption band with a hypsochromic shift[48] demonstrated the active chelation of Th^{4+} ions with the sensor **PHQBA**. Further scrutiny of **PHQBA**'s detection properties with Th^{4+} ions was carried out through the emission titration experiments (Fig. 1b). The gradual addition of thorium ions (0–11 equiv.) to the **PHQBA** solution resulted in the decreased absorption intensity at 380 nm and the subsequent enhancement aroused at 312 nm. The shifts in the absorption bands to produce isosbestic points at 290 and 342 nm revealed the formation of a new complex **PHQBA** + Th^{4+} These findings prove that the sensor **PHQBA** has selective and sensitive detection capability with Th^{4+} ions. To investigate the effect of pH on the detection properties of **PHQBA**, absorption experiments were performed in the presence and absence of Th^{4+} ions. As shown in Fig. S12,† the absorption intensity of **PHQBA** is nearly stable over a broad pH range of 6–12 and shows an enhanced intensity at pH 2–5, likely due to the protonation of the **PHQBA**. Upon the addition of Th^{4+} ions, the absorption intensity of the **PHQBA** + Th^{4+} complex persists stable within the pH range of 6–9 and began to decrease beyond pH 9, due to the hydrolysis of thorium ions. These results indicate that the sensor is capable of responding to Th^{4+} ions across a pH range of 2–12.

Emission studies of PHQBA

Inspired by the absorption experiments, the detection ability of sensor **PHQBA** was examined in ACN/H_2O (8 : 2, v/v) by treating with competing metal ion solutions including Ca^{2+}, Ba^{2+}, Al^{3+}, Cd^{2+}, Cu^{2+}, Th^{4+}, Co^{2+}, Fe^{2+}, Fe^{3+}, Hg^{2+}, Ni^{2+}, Cr^{3+}, Pb^{2+}, Pd^{2+} Zn^{2+}, La^{3+}, and Yb^{3+}. As illustrated in Fig. 2a, the free sensor

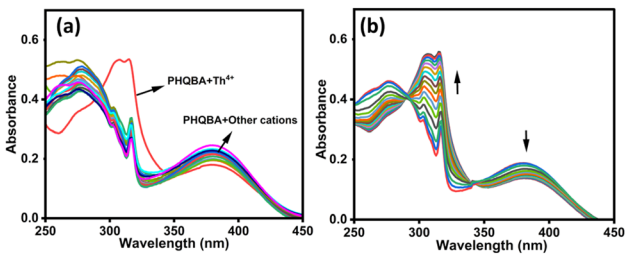

Fig. 1 (a) Absorption spectra of PHQBA (2×10^{-5} M) in the presence of competing cations (1×10^{-4} M); (b) absorption spectra of PHQBA in the presence of varying concentrations of thorium ions (0–11 equiv.).

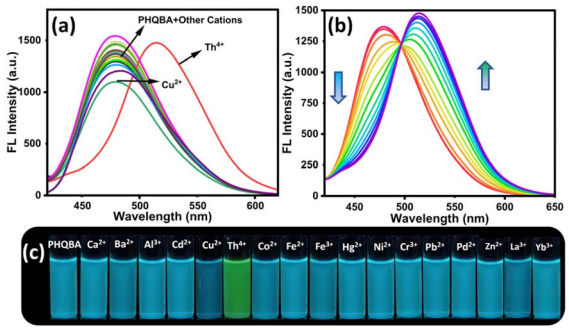

Fig. 2 (a) Fluorescence spectra of **PHQBA** (2×10^{-5} M) in the presence of various cations (1×10^{-4} M); (b) fluorescence spectra of **PHQBA** with the gradual addition of Th^{4+} (0–11 equiv.); (c) emission color changes of **PHQBA** in the presence of series of cations ($\lambda_{ex} = 389$ nm).

PHQBA showed a maximum emission intensity of 478 nm. After the addition of Th^{4+} ions, the emission band at 478 nm redshifted to 515 nm, which could be attributed to the synergic binding of Th^{4+} ion with the sensor **PHQBA**. Notably, other cations did not cause any significant spectral alterations as they led to no discernible binding interactions with the sensor **PHQBA**. To explore the sensitive detection properties of **PHQBA** with Th^{4+} ions, emission titration experiments were performed in ACN/H_2O (8 : 2, v/v) medium. Thereby, the gradual addition of Th^{4+} ions (0–11 equiv.) to the **PHQBA** solution resulted in diminished emission intensity at 478 nm, and the successive emission enhancement was attained at 515 nm (Fig. 2b). The emergence of a clear iso-emissive point at 496 nm indicated the formation of a new complex **PHQBA** + Th^{4+}. As a result, the emission color of **PHQBA** transformed from blue to green (Fig. 2c). The calculated quantum yield values of **PHQBA** and its complex **PHQBA** + Th^{4+} were found to be 0.12 and 0.14 respectively. The slight enhancement in the quantum yield corresponds to the redshifted ratiometric fluorescence of **PHQBA** on chelating with Th^{4+} ions. These findings provided further evidence that sensor **PHQBA** had strong fluorescence detection abilities towards Th^{4+} ions. To clearly distinguish the emission of **PHQBA** and its complex **PHQBA** + Th^{4+}, the chromaticity plot (CIE) was plotted[49] using the emission spectra. As demonstrated in Fig. S8,† the color coordinates of the free probe (**PHQBA**) were found to be in a blue region with the coordinates of $X = 0.145$, $Y = 0.258$, further, the introduction of Th^{4+} the color coordinates of **PHQBA** were shifted towards the green region with the coordinates of $X = 0.215$, $Y = 0.499$. These results denote that **PHQBA** acts as a versatile sensor for the ratiometric detection of Th^{4+} ions. The limit of detection is an essential parameter for evaluating the performance of the chemosensor. The limit of detection was determined by the standard formula 3σ/slope[50] where σ is the standard deviation of blank measurements of **PHQBA** ($n = 10$). The corresponding slope value was obtained from the concentration-dependent linear plot (Fig. S6†). The limit of detection was calculated to be 223 nM, which is comparatively lower than the previously reported thorium sensors (Table S1†). Thus, sensor **PHQBA** can be used as a versatile sensitive tool for the quantitative ratiometric determination of Th^{4+} ions with outstanding sensitivity. Interestingly, the present work relies on evaluating the ratio of fluorescence intensities at two distinct wavelengths (515 and 478 nm). This self-calibration eliminates variations caused by external factors like light source intensity, detector sensitivity, and sample concentration, making the results more robust and reliable.

Interference, reaction kinetics, and pH effect of PHQBA on detecting Th^{4+}

To explore the anti-interference capabilities of **PHQBA** (2×10^{-5}), interference studies were fluorometrically carried out based on the emission ratio of F_{515}/F_{478} nm. The effect of interference was investigated in the presence of various competing cations (1×10^{-4}) such as Ca^{2+}, Ba^{2+}, Al^{3+}, Cd^{2+}, Cu^{2+}, Th^{4+}, Co^{2+}, Fe^{2+}, Fe^{3+}, Hg^{2+}, Ni^{2+}, Cr^{3+}, Pb^{2+}, Pd^{2+}, Zn^{2+}, La^{3+}, and Yb^{3+}. No significant interference was observed. Further, the addition of Th^{4+} ion to the **PHQBA** containing other analyte solutions exhibited enhanced emission intensity in the emission ratio of F_{515}/F_{478} nm, which designates that the sensor **PHQBA**'s sensing capability was sufficient to distinguish Th^{4+} ions from other competing cations and supports the potential identification of Th^{4+} ions coexistence with other cations (Fig. 3a). Further, to explore the influence of pH on the detection properties of **PHQBA**, pH experiments were conducted in the range of 2–12. According to Fig. S11,† the emission of **PHQBA** is consistent across a broad pH range of 6–12 and is observed to be enhanced in an acidic medium spanning from 2–5. The protonation of the N atoms in quinoline and pyridine within the **PHQBA** system may cause increased emission intensity in the acidic medium. On the other hand, thorium(IV) nitrate has the potential to undergo hydrolysis and breakdown when subjected to higher alkaline conditions (11–12). When Th^{4+} ions were added to the **PHQBA** solution, the emission intensity began to increase in the pH range of 6–10 and decreased at pH 11–12. Therefore, the ideal pH range for Th^{4+} ion detection ranges between 6 and 10. The pH-responsive characteristic of the **PHQBA** sensor makes it perfect for detecting Th^{4+} under optimal physiological conditions. Rapid detection of analytes is one of the remarkable characteristics of an ideal chemosensor.[51] For this, time-dependent emission studies were explored. According to Fig. 3b, the free sensor

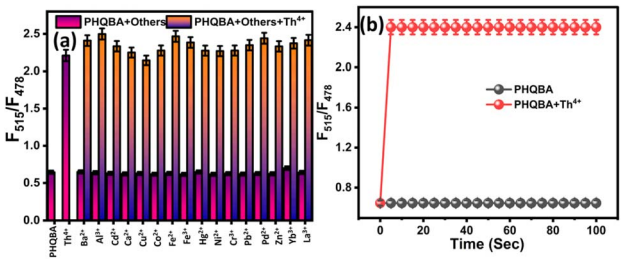

Fig. 3 (a) Interference of **PHQBA** (2×10^{-5} M) in the presence of other cations (1×10^{-4} M) and coexisting with Th^{4+}; (b) time-dependent emission response of **PHQBA** with Th^{4+} ($\lambda_{ex} = 389$ nm).

PHQBA showed feeble emission in the ratio of F_{515}/F_{478} nm. Further, on the addition of Th^{4+} ion to the **PHQBA** solution, the emission intensity significantly elevated within five seconds. Hence, the sensor **PHQBA** was employed as an inevitable tool for the rapid detection of Th^{4+} ions.

Inspection of the detection mechanism

The sensor **PHQBA** encompasses a phenanthridine fluorophore, which is extensively conjugated with thiophene and quinoline moiety. Thus, it produces a blue emissive band. Since the Th^{4+} is electron deficient, it will have a binding interaction with electron-rich heteroatoms [N, N, S] in the **PHQBA** system. By the effect of synergic chelation, sensor **PHQBA** generates distinctive hypsochromic absorption and ratiometric green emission signals with Th^{4+} ions. Moreover, the binding stoichiometry of **PHQBA** with Th^{4+} ions was successively assessed by jobs plot experiments. As depicted in Fig. 4a, the maximum fluorescence intensity was attained when the molar fraction reached 0.5, revealing that the most likely binding mode was a 1 : 1 stoichiometric ratio for the **PHQBA** + Th^{4+} complex. To authenticate the stoichiometric binding of the sensor **PHQBA** with Th^{4+} ions, the Benesi–Hildebrand plot was linearly fitted between $[1/(F_0 - F)]$ and $1/[Th^{4+}]$. The association constant of the formed complex was calculated using the formula: K_a = intercept/slope.[52] The K_a value for **PHQBA** was determined as $3.77 \times 10^5\ M^{-1}$. Such a significant value denotes the robust binding of sensor **PHQBA** with Th^{4+} ions (Fig. 4b).[53] To further understand the coordination mode of **PHQBA** with Th^{4+}, a series of ^1H NMR titration experiments were conducted in DMSO-d_6. As shown in Fig. 4c, the base spectrum represents the free sensor. Upon the sequential addition of Th^{4+} ions (0–11 equivalents), significant changes were observed in the pyridyl proton of **PHQBA** (a) at 9.59 ppm, including a marked decrease in intensity. Furthermore, the incremental addition of Th^{4+} ions induced slight upfield shifts at 8.97 ppm (b), 7.06 ppm (d), and 6.97 ppm (e). A minor upfield shift was also noted for the c proton, which shifted from 8.29 ppm to 8.28 ppm. Notably, the aliphatic protons of **PHQBA** (g, h, and f) were significantly impacted, with their intensities progressively decreasing as the Th^{4+} concentration increased. These observations collectively indicate the effective chelation of Th^{4+} ions by **PHQBA**. Additionally, the mass of the complex was confirmed by high-resolution mass spectroscopy. According to the mass spectral data, the observed mass of the complex **PHQBA** + $Th(NO_3)_4$ was 973.1636, which matched its calculated mass (973.1633) (Fig. S7†). To confirm nitrate binding, we have recorded FTIR spectra. As depicted in Fig. S13,† the observed stretching frequency at 1025 cm^{-1} confirms the presence of NO_3^- in the **PHQBA** + Th^{4+} system.[54]

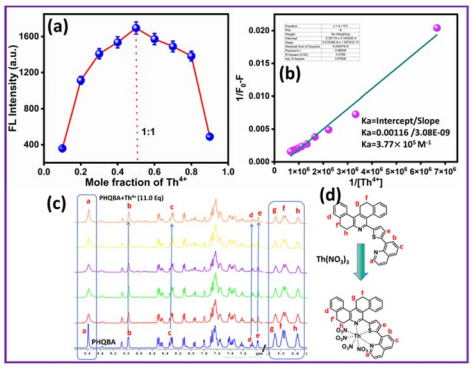

Fig. 4 (a) Jobs plot of **PHQBA** + Th^{4+}; (b) Benesi–Hildebrand plot of **PHQBA** + Th^{4+}; (c) series of ^1H NMR titration spectra of **PHQBA** with Th^{4+} ions (0–11 equiv.).

DFT calculations

To gather clear insights into the theoretical mechanistic aspects of Th^{4+} binding, DFT calculations were performed by employing B3LYP/6-31G*(d,p) levels in Gaussian 16 software.[55–58] For the thorium atom, the SDD basis set was employed[59] as an effective core potential. The optimized electronic structures of **PHQBA** and its complex **PHQBA** + Th^{4+} are depicted in Fig. S10.† In the **PHQBA** + Th^{4+} complex, the receptor **PHQBA** utilizes N atoms of pyridine, quinoline, and sulfur of thiophene to enable efficient chelation with Th^{4+}. The oscillatory strength, *Z*-matrix, calculated energy gap, and frontier molecular orbitals of **PHQBA** and its complex **PHQBA** + Th^{4+} are tabulated in Tables S2–S4.† The frontier molecular orbital images of **PHQBA** and its complex **PHQBA** + Th^{4+} are illustrated in Fig. 5. In the HOMO (highest occupied molecular orbitals) of **PHQBA**, the electron density predominately resided throughout the system, which denotes the higher electron density of the **PHQBA** ligand. In LUMO (lowest unoccupied molecular orbitals) the electron density was located at the phenanthridine skeleton, implying the adequate charge transfer effect in the **PHQBA** system. The calculated energy gap between the HOMO and LUMO orbitals of **PHQBA** was 3.3753 eV. Moreover, in the HOMO of the **PHQBA** + Th^{4+} complex, the phenanthridine thiophene moiety had the enriched electron density, whereas, in the LUMO orbitals, the electron density was predominately found in the quinoline moiety. Further, the calculated energy gap between the HOMO and LUMO of the **PHQBA** + Th^{4+} complex was found to be 3.723 eV, suggesting that the chelation of the Th^{4+} ion effectively enhances the energy gap of the Th^{4+} complex. The introduction of Th^{4+} ions into the detection medium has the potential to alter the local vicinity of **PHQBA** molecules. Such alterations can exert a significant influence on the electronic structure and

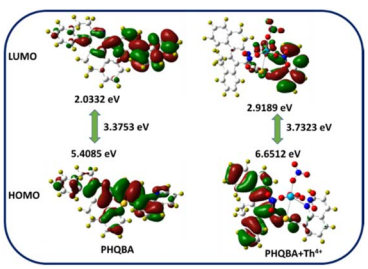

Fig. 5 The frontier molecular orbitals of **PHQBA** and **PHQBA** + Th^{4+} complex.

optical characteristics of the material. Perturbations in the environmental conditions can lead to shifts in the energy levels associated with electronic transitions, thereby inducing a red shift in emission.[60,61] Concurrently, the overall band gap of the **PHQBA** + Th^{4+} complex may increase as a consequence of the perturbed electronic structure induced by the surrounding medium. Based on this ratiometric fluorescence sensing mechanism, the frontier molecular orbitals are mainly distributed at quinoline moiety in the Th^{4+} complex, while the excited electron of the nitrogen unit is back to the ground state resulting in ratiometric fluorescence. These findings denote that sensor **PHQBA** could synergically coordinate with the Th^{4+} atom to form a 1 : 1 stoichiometric complex with the sensor **PHQBA**.

Portable test strips aided detection

Portable test strip facilitated detection is a facile and intellectual approach for the visual discrimination of target analytes.[62] In our endeavor to assess the practical value of **PHQBA**, portable test strip experiments have been conducted in our laboratory. The selectivity of **PHQBA** (2×10^{-5}) in the presence of various ion solutions (1×10^{-4}) such as Ca^{2+}, Ba^{2+}, Al^{3+}, Cd^{2+}, Cu^{2+}, Co^{2+}, Fe^{2+}, Fe^{3+}, Hg^{2+}, Ni^{2+}, Cr^{3+}, Pb^{2+}, Pd^{2+}, Zn^{2+}, La^{3+}, and Yb^{3+} were tested appropriately. When seen under the illumination of UV-365 nm, **PHQBA** showed a remarkable selectivity to Th^{4+} ions over other cations. Only after the exposure of Th^{4+} ions, the blue emission of **PHQBA** altered to green, as shown in Fig. 6. However, other cation solutions did not show appreciable emission changes in the **PHQBA**-impregnated strips. Hence, it can be used as a portable sensor for the ratiometric discrimination of Th^{4+} ions.

Reproducible nature of PHQBA

Reversibility and reusability are characteristic features of a noble chemosensor. In this regard, the reproducible properties of **PHQBA** were explored in ACN/H_2O (8 : 2, v/v). Sensor **PHQBA** demonstrated an intensive emission band at 478 nm, which produced a characteristic blue fluorescence. Then, the addition of Th^{4+} ions to the **PHQBA** solution resulted in ratiometric green fluorescence. Since ethylenediaminetetraacetic acid (EDTA) is a potential chelating agent,[63] Th^{4+} ion-facilitated ratiometric fluorescence was substantially reversed by the subsequent additions of EDTA. As depicted in Fig. 7, the emission changes were incredibly imitated in fluorescence spectra, in which the introduction of EDTA solution in the **PHQBA** + Th^{4+} complex, resulted in the regeneration of the probe's emission at 478 nm. These outcomes imply that the Th^{4+} ion has been significantly eradicated from the sensor and that it finely achieves the reversibility process induced by the efficient interaction of EDTA with the **PHQBA** + Th^{4+} complex. These reproducible and reversible processes (blue to green fluorescence) were repeated for 4 cycles (Fig. S9†) with successive alternative additions of Th^{4+} and EDTA. The outcomes revealed that the sensor **PHQBA** can be reused and also sensitively employed for the detection of Th^{4+} ions.

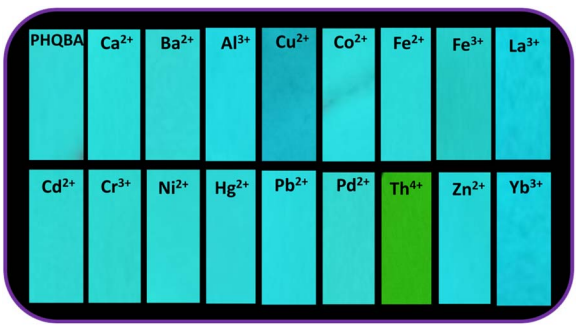

Fig. 6 PHQBA (2×10^{-5}) impregnated test strips for Th^{4+} ion (1×10^{-4}) detection.

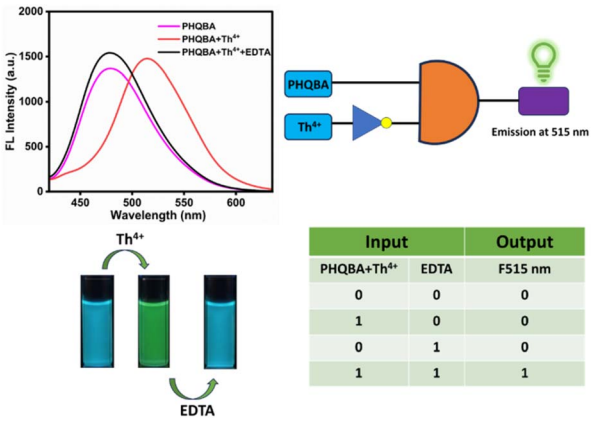

Input		Output
PHQBA+Th^{4+}	EDTA	F515 nm
0	0	0
1	0	0
0	1	0
1	1	1

Fig. 7 Reversibility studies of PHQBA in the presence of Th^{4+} with EDTA and their logic gates representation.

Real-time applications

The versatile sensing properties of **PHQBA** inspired us to explore its practical efficacy in various environmental water samples.[64] The known concentration of Th^{4+} ion solution was spiked with realistic water samples (drinking water, lake water, and tap water collected from Vellore). Then the experiment was repeated three times with each sample. The average recoveries and relative standard deviations (R. S. D.) of the corresponding spiked samples are tabulated in Table 1. As represented in Table 1, the average recoveries of various water samples ranged from 90.1 to 98.5%, and the corresponding relative standard deviation values were found to be 0.97 to 1.19%.

Table 1 Tabulation of real water sample analysis[a]

Sample	Added (μM)	Found (μM)	Recovery (%)	RSD (%)
Lake water	0.5	0.46	92.2	1.01
	1.0	0.90	90.1	0.97
Tap water	0.5	0.47	94.3	0.99
	1.0	0.96	96.5	1.19
Drinking water	0.5	0.49	98.5	1.09
	1.0	0.97	97.6	1.11

[a] Samples were collected in and around Vellore.

Based on these analytical findings, sensor **PHQBA** was effectively applied to determine Th^{4+} ion in real water samples with reliability and accuracy. Hence, the sensor **PHQBA** emerged as a valuable candidate for the real-time analysis of Th^{4+} ions in real water samples.

Conclusion

A new phenanthridine-derived quinoline-based fluorescent sensor was successfully developed for the ratiometric discrimination of Th^{4+} ions. On interaction with Th^{4+} ions, the emission of **PHQBA** ratiometrically changed from blue to green with the facilitation of chelation enhanced fluorescence process. The versatile sensing properties of **PHQBA** endorse hypsochromic absorption, and the redshifted emission bands during the interaction with Th^{4+} were thoroughly investigated by absorption and emission experiments. The binding interaction of Th^{4+} ions with **PHQBA** was explored by ^1H NMR, HRMS, and DFT analysis. The portable test strips confirmed that the sensor **PHQBA** can selectively detect Th^{4+} ions without the aid of any sophisticated instrumental facility. Also, the sensor **PHQBA** was analyzed for the real-time detection of Th^{4+} ions in real water samples. The versatile features of **PHQBA** such as reversibility/reusability, selectivity, and practical utility will accelerate the advancement of fluorescent sensors in adaptable analytical applications. Developing ultrasensitive chemosensors for the detection of radioactive ions is a critical research area with extensive implications in environmental monitoring, nuclear safety, and non-proliferation initiatives. Systematic monitoring of thorium ions is particularly essential to ensure compliance with nuclear regulations and to safeguard public health and safety. Advanced tools capable of detecting ultra-low concentrations of thorium in soil, water, and air are crucial for identifying contamination and assessing its environmental impact. In our laboratory, ongoing research focuses on innovative structural modifications to develop highly sensitive detection methods capable of identifying radioactive elements at extremely low concentrations. These advanced analytical techniques aim to significantly enhance the accuracy, sensitivity, and efficiency of analyte detection, even in complex and challenging environments, thereby paving the way for more effective and reliable monitoring solutions in the future.

Data availability

The data supporting this article have been included as part of the ESI.†

Conflicts of interest

The authors declare no financial interests.

Acknowledgements

Selin Manoj Kumar sincerely thanks Vellore Institute of Technology for providing a Teaching Cum Research Assistant (Project No.: VIT/HR/2022/19062). The DST-FIST NMR facility at VIT University is duly acknowledged. Finally, the authors thank Dr R. Srinivasan, SSL-VIT, for language editing.

References

1 M. Cuney, *Non-Renewable Resource Issues: Geoscientific and Societal Challenges*, 2012, pp. 91–129.
2 M. Corn, *Handbook of Hazardous Materials*, Academic Press, 2012.
3 C. S. K. Raju and M. Subramanian, *J. Hazard. Mater.*, 2007, **145**, 315–322.
4 S. Yang, N. Tan, X. Yan, F. Chen, W. Long and Y. Lin, *Mar. Pollut. Bull.*, 2013, **74**, 213–219.
5 S. Yang, N. Tan, X. Yan, F. Chen, W. Long and Y. Lin, *Mar. Pollut. Bull.*, 2013, **74**, 213–219.
6 D. Brugge, J. L. deLemos and B. Oldmixon, *Rev. Environ. Health*, 2005, **20**, 177–194.
7 E. Zambrzycka-Szelewa and B. Godlewska-Zylkiewicz, *Spectrochim. Acta, Part B*, 2024, **213**, 106859.
8 M. Ioannidou, G. Zachariadis, A. Anthemidis and J. Stratis, *Talanta*, 2005, **65**, 92–97.
9 A. M. Clark, A. D. Nelson, T. L. Bailey, D. Blankstein, C. Boomershine, G. M. Brown, P. C. Burns, S. Carmichael, L. K. Callahan and J. Koros, *Nucl. Instrum. Methods Phys. Res., B*, 2024, **548**, 165253.
10 X. Qiu, Z. Hu, T. He, T. Luo, W. Zhang, M. Li, K. Zong, Z. Wang and Y. Liu, *J. Anal. At. Spectrom.*, 2024, **39**, 545–557.
11 J. Sardans, F. Montes and J. Peñuelas, *Spectrochim. Acta, Part B*, 2010, **65**, 97–112.
12 M. Ghosh, M. Sarma, S. Dagupta, J. Datta and K. Swain, *Anal. Chem. Lett.*, 2024, **14**, 382–394.
13 K. P. Carter, A. M. Young and A. E. Palmer, *Chem. Rev.*, 2014, **114**, 4564–4601.
14 A. P. De Silva, H. N. Gunaratne, T. Gunnlaugsson, A. J. Huxley, C. P. McCoy, J. T. Rademacher and T. E. Rice, *Chem. Rev.*, 1997, **97**, 1515–1566.
15 M. Dutta and D. Das, *TrAC, Trends Anal. Chem.*, 2012, **32**, 113–132.
16 T. Rasheed, M. Bilal, F. Nabeel, H. M. Iqbal, C. Li and Y. Zhou, *Sci. Total Environ.*, 2018, **615**, 476–485.
17 D. Jothi, S. Munusamy, S. Enbanathan and S. K. Iyer, *RSC Adv.*, 2022, **12**, 8570–8577.
18 S. M. Kumar, D. Jothi, S. Munusamy, S. Enbanathan and S. K. Iyer, *J. Photochem. Photobiol. Chem.*, 2023, **434**, 114269.
19 Z. Aydin, *J. Turk. Chem. Soc., Sect. A*, 2020, **7**, 277–286.
20 X. M. Wang, H. Yan, Y. Chen and H. B. Bao, *Adv. Mater. Res.*, 2011, **239**, 1105–1108.
21 D. Mohanasundaram, R. Bhaskar, G. G. V. Kumar, J. Rajesh and G. Rajagopal, *Microchem. J.*, 2021, **164**, 106030.
22 H.-I. Un, C.-B. Huang, C. Huang, T. Jia, X.-L. Zhao, C.-H. Wang, L. Xu and H.-B. Yang, *Org. Chem. Front.*, 2014, **1**, 1083–1090.
23 L. Gao, C. Deng, J. Xiong, P. Zhu, Q. Chen and K. Tan, *Microchem. J.*, 2019, **150**, 104096.
24 Z. Zhang, J. Feng, P. Huang, S. Li and F.-Y. Wu, *Sens. Actuators, B*, 2019, **298**, 126891.

25 G. Lu, Z. Jia, M. Yu, M. Zhang and C. Xu, *Molecules*, 2023, **28**, 7818.
26 M. Royzen, Z. Dai and J. W. Canary, *J. Am. Chem. Soc.*, 2005, **127**, 1612–1613.
27 H. Wang, H. Xing, W. Liu, Y. Hao, L. Zhang, Z. Yang, Q. Hu, S. Shuang, C. Dong and X. Gong, *Sens. Actuators, B*, 2022, **352**, 130991.
28 N. Tohora, S. Ahamed, M. Mahato, J. Chourasia, S. Ali and S. K. Das, *J. Photochem. Photobiol. Chem.*, 2024, **457**, 115921.
29 Y. Li, L. Li, X. Pu, G. Ma, E. Wang, J. Kong, Z. Liu and Y. Liu, *Bioorg. Med. Chem. Lett.*, 2012, **22**, 4014–4017.
30 M. Gao, P. Xie, L. Wang, X. Miao and F. Guo, *Res. Chem. Intermed.*, 2015, **41**, 9673–9685.
31 Y. Chen, F. Li and Z. Bo, *Macromolecules*, 2010, **43**, 1349–1355.
32 S. Yashmin, S. Mondal, R. Das, P. Banerjee and A. T. Khan, *Org. Biomol. Chem.*, 2022, **20**, 7302–7315.
33 D. Wu, B. Fang, M. Zhang, W. Du, J. Zhang, X. Tian, Q. Zhang, H. Zhou, J. Wu and Y. Tian, *Dyes Pigm.*, 2018, **159**, 142–150.
34 S. Karthik, J. Ajantha, S. Easwaramoorthi and T. Gandhi, *New J. Chem.*, 2020, **44**, 9530–9539.
35 R. M. Gadirov, L. G. Samsonova, K. M. Degtyarenko, A. E. Kurtsevich, I. K. Yakushchenko and T. N. Kopylova, *J. Fluoresc.*, 2021, **31**, 1333–1342.
36 S. Swaminathan, S. Munusamy, D. Jothi and S. K. Iyer, *ChemistrySelect*, 2021, **6**, 858–864.
37 L. Liu, L. Ga and J. Ai, *Biosens. Bioelectron.*, 2022, **213**, 114456.
38 S. M. Kumar, S. Munusamy, S. Manickam, D. Jothi, S. Enbanathan and S. K. Iyer, *J. Mol. Liq.*, 2023, **381**, 121828.
39 X. Pei, Y. Pan, L. Zhang and Y. Lv, *Appl. Spectrosc. Rev.*, 2021, **56**, 324–345.
40 S. Manoj Kumar and S. Kulathu Iyer, *J. Org. Chem.*, 2024, **89**, 5392–5400.
41 S. Enbanathan, S. Munusamy, D. Jothi, S. Manojkumar, S. Manickam and S. K. Iyer, *RSC Adv.*, 2022, **12**, 27839–27845.
42 S. Seenan and K. I. Sathiyanarayanan, *Inorg. Chem. Commun.*, 2021, **132**, 108825.
43 S. Sawminathan and S. K. Iyer, *Spectrochim. Acta, Part A*, 2022, **265**, 120403.
44 D. Jothi, S. Manickam, S. Sawminathan, S. Munusamy, S. A. Kumar and S. K. Iyer, *Dyes Pigm.*, 2022, **197**, 109826.
45 W. Li, Y. Fu, T. Liu, H. Li and M. Huang, *Spectrochim. Acta, Part A*, 2023, **288**, 122147.
46 N. N. Zhadin and R. R. Alfano, *J. Biomed. Opt.*, 1998, **3**, 171–186.
47 S. Srinivas and R. Mutharasan, *Biotechnol. Bioeng.*, 1987, **30**, 769–774.
48 A. Elabd, *RSC Adv.*, 2016, **6**, 45525–45532.
49 R. Yao, Z. Li, G. Liu, C. Fan and S. Pu, *Talanta*, 2021, **234**, 122612.
50 S. M. Kumar, D. Jothi, S. Munusamy, S. Enbanathan and S. K. Iyer, *J. Photochem. Photobiol. Chem.*, 2023, **434**, 114269.
51 N. Duan, S. Yang, H. Tian and B. Sun, *Food Chem.*, 2021, **358**, 129839.
52 S. M. Kumar, S. Munusamy, S. Manickam, D. Jothi, S. Enbanathan and S. K. Iyer, *J. Mol. Liq.*, 2023, **381**, 121828.
53 R. Wang and Z. Yu, *Acta Phys.-Chim. Sin.*, 2007, **23**, 1353–1359.
54 A. Knyazev, G. Fukin, R. Rumyantcev, M. Komshina, I. Savushkin and A. Paranyuk, *Polyhedron*, 2016, **117**, 600–603.
55 B. Pavankumar, P. Ranjan, R. R. Panicker, P. C. Jha, C. Brahmananda Rao, R. Desikan and A. Sivaramakrishna, *ChemistrySelect*, 2024, **9**, e202304509.
56 J. E. Del Bene, W. B. Person and K. Szczepaniak, *J. Phys. Chem.*, 1995, **99**, 10705–10707.
57 H. Kruse, L. Goerigk and S. Grimme, *J. Org. Chem.*, 2012, **77**, 10824–10834.
58 M. P. Andersson and P. Uvdal, *J. Phys. Chem.*, 2005, **109**, 2937–2941.
59 R. Sk, S. A. Kumar, K. Vijayakrishna, A. Sivaramakrishna, C. V. S. B. Rao, N. Sivaraman and S. K. Sahoo, *Inorg. Chem.*, 2018, **57**, 15270–15279.
60 S. Seenan, S. Manickam, S. Sawminathan, D. Jothi and S. K. Iyer, *J. Photochem. Photobiol. Chem.*, 2022, **430**, 113952.
61 S. Sawminathan and S. K. Iyer, *New J. Chem.*, 2021, **45**, 6033–6041.
62 Y. Shen, Y. Wei, C. Zhu, J. Cao and D.-M. Han, *Coord. Chem. Rev.*, 2022, **458**, 214442.
63 S. M. Kumar, S. Munusamy, D. Jothi, S. Enbanathan and S. K. I. Iyer, *J. Mol. Liq.*, 2023, **373**, 121235.
64 S. M. Kumar, S. Munusamy, D. Jothi, S. Enbanathan, J. Haribabu and S. K. Iyer, *Opt. Mater.*, 2023, **144**, 114382.